

Sol–Gel Synthesis of Oxygen-Ion Conductors Based on Apatite-Structure Silicates and Silicophosphates

A. V. Teterskii, S. Yu. Stefanovich, and N. Ya. Turova

Moscow State University, Vorob'evy gory 1, Moscow, 119899 Russia

e-mail: stefan@tech.chem.msu.ru

Received September 22, 2005

Abstract—Oxygen-ion-conducting orthosilicates were synthesized for the first time by a sol–gel process. Apatite-structure compounds with the general formula $M_2^{\text{II}}\text{Ln}_8(\text{SiO}_4)_6\text{O}_2$ ($M^{\text{II}} = \text{Ca, Sr, Pb; Ln} = \text{La, Pr, Nd, Gd, Er, Yb}$) were prepared by reacting tetraethyl orthosilicate, $\text{Si}(\text{OEt})_4$, with divalent-metal ethoxides or nitrates and rare-earth nitrates in aqueous–ethanolic solutions. The formation of oxide phases during heat treatment of xerogels obtained by a sol–gel process was studied. By sintering ground xerogels, high-strength, pore-free ceramics were prepared, which are superior to ceramics prepared through standard solid-state reactions in electrical properties and microstructure and are close in conductivity to single-crystal analogs.

DOI: 10.1134/S0020168506030150

INTRODUCTION

Ionic membrane technology employing high-temperature solid oxide fuel cells is presently considered the most attractive approach to the direct conversion of the chemical energy of natural methane to electric energy on a commercial scale [1–5]. The basic requirement of the electrolyte material for this application is that it combine high oxygen-ion mobility with good chemical stability and mechanical strength at temperatures on the order of 1000°C in a broad range of redox potentials. The electrolyte material for industrial application must be prepared in the form of a vacuum-tight coating less than 100 μm in thickness on a porous ceramic support. In spite of the considerable effort concentrated on the search for effective oxygen-ion conductors and optimization of their synthesis, no commercially viable approach to this problem has been proposed to date.

It is reasonable to expect that considerable improvements in the technology of the materials in question can be achieved by using solution-phase processes instead of solid-state reactions. Such processes typically ensure a more perfect crystal structure and microstructure of polycrystalline materials at lower synthesis and sintering temperatures [6] and are better suited for producing coating. Unfortunately, the known approaches to the synthesis of the most widespread oxygen-ion conductors based on ZrO_2 [7] and LaGaO_3 [8–10] from nitrates or carboxylates have had limited success, especially in the preparation of monolithic solid-electrolyte coatings with optimal thicknesses for practical application, 10–30 μm [11].

In this paper, we examine the possibility of using the sol–gel method for the synthesis of promising orthosilicates with the general formula $M_2^{\text{II}}\text{Ln}_8(\text{SiO}_4)_6\text{O}_2$ ($M^{\text{II}} = \text{Ca, Sr, Pb; Ln} = \text{La, Pr, Nd, Gd, Er, Yb}$) and related apatite-structure rare-earth silicates and silicophosphates. Ceramic and single-crystal samples of some silicates and silicophosphates in this family have been recently reported to possess high oxygen ionic conductivity [12, 13].

EXPERIMENTAL

$M_2^{\text{II}}\text{Ln}_8(\text{SiO}_4)_6\text{O}_2$ orthosilicates were synthesized by a sol–gel process from tetraethyl orthosilicate ($\text{Si}(\text{OEt})_4$, TEOS) and metal alkoxides and nitrates. In addition, ammonium dihydrogen phosphate was used in the synthesis of silicophosphates.

The apatite-structure $M_2^{\text{II}}\text{Ln}_8(\text{SiO}_4)_6\text{O}_2$ ($M^{\text{II}} = \text{Ca, Sr, Pb; Ln} = \text{La, Pr, Nd, Gd, Er, Yb}$) orthosilicates were prepared by reacting divalent-metal alkoxides or nitrates with rare-earth nitrates and TEOS in acid solutions containing water and ethanol at an $M^{\text{II}} : \text{Ln} : \text{Si}$ atomic ratio of 2 : 8 : 6. $\text{Ca}(\text{OEt})_2 \cdot 4\text{EtOH}$ and $\text{Sr}(\text{OEt})_2 \cdot 4\text{EtOH}$ ethoxide solutions were prepared by reacting metals with absolute ethanol as described earlier [14]. Immediately before synthesis, $\text{Si}(\text{OEt})_4$ (reagent grade, Penta) was subjected to fractional distillation, and the fraction with a boiling point of 170°C was used subsequently. The $M^{\text{II}}(\text{NO}_3)_2$ and $\text{Ln}(\text{NO}_3)_3$ nitrates were prepared by dissolving analytical-grade

carbonates and oxides, respectively, in concentrated nitric acid.

Below, we describe three procedures for the preparation of reaction solutions differing in composition, illustrated by the example of Nd-containing silicates and silicophosphates. In all preparations, TEOS was used as a siliceous gelation agent, and distilled water was boiled or 1 h to remove CO₂.

Procedure I (nitrates and ethoxides). Calcium metal (0.214 g, 5.349 mmol) was dissolved in absolute ethanol (20 ml) at room temperature, and then a solution of Si(OEt)₄ (3.338 g, 16.048 mmol) in ethanol (10 ml) was added. Next, an acid solution of Nd(NO₃)₃ heated to 50–60°C was added while vigorously stirring. The latter solution was prepared by dissolving Nd₂O₃ (3.599 g, 10.698 mmol) in concentrated nitric acid.

Procedure II (M(NO₃)₂ and Ln(NO₃)₃ nitrates). Nd₂O₃ (1.515 g, 4.502 mmol) and CaCO₃ (0.2643 g, 2.641 mmol) were dissolved in concentrated HNO₃ (10 ml), and the solution was diluted with 20 ml of H₂O. Next, a solution of Si(OEt)₄ (1.648 g, 7.923 mmol) in ethanol (10 ml) was added while vigorously stirring, and the reaction mixture was heated to 50–60°C to accelerate hydrolysis.

Procedure III (nitrates and phosphates). To synthesize the silicophosphate Ca₃Nd₇(SiO₄)₅(PO₄)O₂, we used a solution of Nd₂O₃ (1.8502 g, 5.498 mmol) and CaCO₃ (0.27517 g, 2.749 mmol) in concentrated HNO₃. To the nitrate solution was added Si(OEt)₄ (1.635 g, 7.855 mmol) in ethanol (5 ml). To avoid precipitation of calcium and rare-earth phosphates during the preparation of silicophosphate compounds, a solution of NH₄H₂PO₄ (0.1806 g, 1.571 mmol) in distilled water (5 ml) was added to acid nitrate solutions prepared as described above.

The solutions were boiled down on a water bath to a volume of ≈10–15 ml, which led to an increase in their viscosity and gelation. During subsequent heat treatment at 300°C for 1–1.5 h, the gel converted to amorphous xerogel. To establish the crystallization sequence of the xerogel, it was thoroughly ground and then annealed (for 2 h) consecutively at 500, 650, 800, 900, 1000, and 1100°C. After each step, the material was characterized by powder x-ray diffraction (XRD) analysis.

The resultant crystalline powder was used to prepare disk-shaped ceramic samples. To increase the green density, two or three drops of ethanol were added to the powder before pressing. The powder was pressed at 3–4 MPa, and the green compacts were fired at 1300–1470°C for 1 h.

XRD studies were carried out at room temperature with a Termo ARL X'TRA diffractometer (CuK_{α1} radiation, λ = 1.54060 Å, 2θ = 10°–60°, scan step of 0.02°). After sintering, XRD characterization was repeated. In electrical measurements, we used disks 6–7 mm in

diameter and 1–2 mm in thickness. Electrical contacts to the faces of the samples were made by firing colloidal platinum paste. The real and imaginary parts of electrical conductivity were measured by a two-probe method at frequencies from 10 Hz to 1 MHz and temperatures from 20 to 1000°C, using a computer-controlled ac bridge.

The microstructure of ceramic samples was examined by scanning electron microscopy (SEM) on a JEOL JEM-2000FXII. Magnification was adjusted so as to observe morphological features 0.5 to 20 μm in size.

RESULTS AND DISCUSSION

Formation of apatite-like silicates and silicophosphates. Using procedures I–III and aqueous–ethanolic solutions of nitrates (or alkoxides) and TEOS we obtained gels, which were then heat-treated and annealed to give phase-pure apatite-structure M^{II}Ln₈(SiO₄)₆O₂ and Ln_{9.33}(SiO₄)₆O₂ (M^{II} = Ca, Sr, Pb; Ln = La, Pr, Nd, Gd, Er) orthosilicates. The crystallization of all the phases reached completion near 1100°C.

The synthesis conditions and the main physicochemical properties of the synthesized single- and mixed-phase apatite-like materials are summarized in Table 1. Using the sol-gel method, we were able to obtain, in single-phase form, all of the M^{II}Ln₈(SiO₄)₆O₂ (M^{II} = Ca, Sr; Ln = light rare earths) compounds prepared in earlier studies by solid-state reactions. Attempts to synthesize ytterbium orthosilicates were unsuccessful: all of the samples contained impurity phases, in particular Yb₂O₃. Note that only every sixth SiO₄ group in the apatite-like structure could be replaced with a PO₄ group when ammonium dihydrogen phosphate was added to the starting nitrate solution. The introduction of a larger amount of PO₄ groups led to the formation of a mixture of apatite and LnPO₃.

None of the synthesized orthosilicates or silicophosphates close in stoichiometry to apatite, (M^{II},Ln)_x(XO₄)₇ with X = P, Si and x = 9–10.5, contained a whitlockite (phosphorus-rich) or cerite (silicon-rich) phase. Instead, the samples contained apatite-structure phases and SiO₂ (5–10%). This result indicates that, under the conditions of this study, cerite cannot be synthesized. Indeed, high-temperature annealing of xerogel rules out the presence of hydroxyls, which are known to stabilize (Ln,M²⁺)_{9.7}((Si,P)O₄)₆(OH)_{2.8} [15] under hydrothermal conditions.

By sintering ground xerogels, we obtained conductive, high-strength, pore-free ceramics with apatite-like structures: Ca₂Ln₈(SiO₄)₆O₂, Sr₂Ln₈(SiO₄)₆O₂, Pb₂Ln₈(SiO₄)₆O₂, and Ln_{9.33}(SiO₄)₆O₂ (Ln = La–Er).

Table 1. Sol–gel synthesis conditions and the main physicochemical properties of apatite-structure compounds

Cation ratio	Synthesis procedure	Heat-treatment conditions: $t, ^\circ\text{C}/\tau, \text{h}$	Phase composition	Lattice parameters, \AA	$\sigma, \text{S/cm}$ (900 $^\circ\text{C}$)	E_a, eV
Ca : La : Si = 2 : 8 : 6	I, II	300/1.5	Amorphous phase	$a = b = 9.651,$ $c = 7.151 (V = 576.8 \text{\AA}^3)$	4.16×10^{-6}	1.12
		1100/2	$\text{Ca}_2\text{La}_8(\text{SiO}_4)_6\text{O}_2^{**}$			
Sr : La : Si = 2 : 8 : 6	II	300/1	–	$a = b = 9.708,$ $c = 7.238 (V = 590.76 \text{\AA}^3)$	9.26×10^{-6}	0.89
		1100/2	$\text{Sr}_2\text{La}_8(\text{SiO}_4)_6\text{O}_2^{**}$			
Pb : La : Si = 2 : 8 : 6*	II	300/1	Amorphous phase	$a = b = 9.725,$ $c = 7.249 (V = 593.75 \text{\AA}^3)$	4.09×10^{-5}	1.19
		1100/2	$\text{Pb}_2\text{La}_8(\text{SiO}_4)_6\text{O}_2^{**}$			
La : Si = 9.33 : 6	II	300/1	–	$a = b = 9.723,$ $c = 7.1895 (V = 588.83 \text{\AA}^3)$	6.74×10^{-4}	0.71
		1100/2	$\text{La}_{9.33}(\text{SiO}_4)_6\text{O}_2$			
Sr : Pr : Si = 2 : 8 : 6*	II	300/3	Amorphous phase	$a = b = 9.607,$ $c = 7.139 (V = 570.61 \text{\AA}^3)$	8.53×10^{-6}	1.40
		1000/10	$\text{Sr}_2\text{Pr}_8(\text{SiO}_4)_6\text{O}_2^{**}$			
Ca : Nd : Si = 2 : 8 : 6	I, II	300/3	Amorphous phase	$a = b = 9.532,$ $c = 7.021 (V = 552.45 \text{\AA}^3)$	2.64×10^{-6}	1.18
		500/5	Amorphous phase			
		800/1	Amorphous phase			
		1000/10	$\text{Ca}_2\text{Nd}_8(\text{SiO}_4)_6\text{O}_2^{**}$			
Sr : Nd : Si = 2 : 8 : 6	II	300/1	Amorphous phase	$a = b = 9.566,$ $c = 7.106 (V = 563.14 \text{\AA}^3)$	8.00×10^{-6}	0.86
		1100/2	$\text{Sr}_2\text{Nd}_8(\text{SiO}_4)_6\text{O}_2^{**}$			
Pb : Nd : Si = 2 : 8 : 6	II	300/10	–	$a = b = 9.601,$ $c = 7.105 (V = 567.12 \text{\AA}^3)$	3.48×10^{-5}	0.88
		1000/5	$\text{Pb}_2\text{Nd}_8(\text{SiO}_4)_6\text{O}_2^{**}$			
Ca : Gd : Si = 2 : 8 : 6	I, II	300/1	–	$a = b = 9.421,$ $c = 6.888 (V = 529.44 \text{\AA}^3)$	3.42×10^{-6}	1.39
		1000/2	$\text{Ca}_2\text{Gd}_8(\text{SiO}_4)_6\text{O}_2^{**}$			
$\text{Nd}_{9.33}(\text{SiO}_4)_6\text{O}_2$	I	300/1	–	$a = b = 9.571,$ $c = 7.024 (V = 557.28 \text{\AA}^3)$	5.52×10^{-4}	0.69
		1100/2	$\text{Nd}_{9.33}(\text{SiO}_4)_6\text{O}_2$			
Sr : Gd : Si = 2 : 8 : 6	II	300/1	–	$a = b = 9.463,$ $c = 6.971 (V = 540.61 \text{\AA}^3)$	7.62×10^{-6}	1.18
		1000/2	$\text{Sr}_2\text{Gd}_8(\text{SiO}_4)_6\text{O}_2^{**}$			
Ca : Er : Si = 2 : 8 : 6*	I, II	300/5	–	$a = b = 9.310,$ $c = 6.757 (V = 507.23 \text{\AA}^3)$	2.41×10^{-6}	1.23
		1000/10	$\text{Ca}_2\text{Er}_8(\text{SiO}_4)_6\text{O}_2^{**}$			
Sr : Er : Si = 2 : 8 : 6	II	300/2	–	$a = b = 9.346,$ $c = 6.826 (V = 516.35 \text{\AA}^3)$	6.75×10^{-6}	0.98
		1100/2	$\text{Sr}_2\text{Er}_8(\text{SiO}_4)_6\text{O}_2^{**}$			
Pb : Er : Si = 2 : 8 : 6	II	300/2	–	$a = b = 9.461,$ $c = 6.830 (V = 529.40 \text{\AA}^3)$	1.62×10^{-5}	1.10
		1100/2	$\text{Pb}_2\text{Er}_8(\text{SiO}_4)_6\text{O}_2^{**}$			
Ca : Yb : Si = 2 : 8 : 6*	II	300/5	–	–	–	–
		900/6	AP** + CaSiO_3 + Yb_2O_3 + SiO_2			
Sr : Yb : Si = 2 : 8 : 6*	II	300/5	Amorphous phase	–	–	–
		900/6	–			
Yb : Si = 9.33 : 6	II, III	1000/10	AP** + Yb_2O_3	–	–	–
		300/1	–			
		1100/2	AP** + Yb_2O_3	–	–	–

Table 1. (Contd.)

Cation ratio	Synthesis procedure	Heat-treatment conditions: $t, ^\circ\text{C}/\tau, \text{h}$	Phase composition	Lattice parameters, \AA	$\sigma, \text{S/cm}$ (900 $^\circ\text{C}$)	E_a, eV
Ca : Nd : Si = 2 : 8 : 6	I	300/5	Amorphous phase	—	—	—
		500/10	Amorphous phase			
		650/5	Amorphous phase			
		900/10	$\text{Ca}_2\text{Nd}_8(\text{SiO}_4)_6\text{O}_2^{**}$ + SiO_2			
Mg : Nd : Si = 2 : 8 : 7	II	1000/5	$\text{Mg}_2\text{Nd}_8(\text{SiO}_4)_6\text{O}_2^{**}$ + <5% SiO_2	—	—	—
Ca : Er : Si = 2 : 8 : 7	II	300/3	—	—	—	—
		1000/15	$\text{Ca}_2\text{Er}_8(\text{SiO}_4)_6\text{O}_2^{**}$ + 5% SiO_2	—	—	—
Ca : Nd : Si : P = 3 : 7 : 5 : 1	III	300/2	—	$a = b = 9.505,$ $c = 6.9991$ ($V = 547.62 \text{ \AA}^3$)	5.75×10^{-6}	1.31
		1000/3	$\text{Ca}_3\text{Nd}_7(\text{SiO}_4)_5(\text{PO}_4)\text{O}_2^{**}$			
Ca : Nd : Si : P = 2 : 8 : 4 : 2	III	300/1	—	—	—	—
		1100/2	AP** + NdPO_4	—	—	—
Ca : La : Si : P = 2 : 8 : 4 : 2	III	300/1	—	—	—	—
		1100/3	AP** + LaPO_4	—	—	—
La : Si : P = 9.33 : 4 : 2	III	300/2	—	—	—	—
		1100/3	AP** + LaPO_4	—	—	—
La : Si : P = 9 : 5 : 1	III	300/1	—	—	—	—
		1000/2	AP** + La_2O_3 + LaPO_4	—	—	—

* The compound was also prepared by solid-state synthesis.

** Apatite-structure phase.

The density of the ceramics, determined by the buoyancy method using a Thoulet solution ($\rho = 3.827 \text{ g/cm}^3$) as the buoyancy fluid, was 92–97% of theoretical density.

Microstructures of ceramics. Figure 1 shows the surface microstructures of two $\text{Ca}_2\text{Nd}_8(\text{SiO}_4)_6\text{O}_2$ ceramic samples prepared through sol-gel processing and solid-state reactions. The sintering temperatures were 1400 and 1600 $^\circ\text{C}$, respectively (Table 2). The porosity of the sol-gel-derived ceramic is lower than that of the material prepared through solid-state reaction, in agreement with density measurements. In addition, the sol-gel-derived ceramic is more uniform in grain size.

Electrical conductivity and dielectric properties. Figure 2 shows the temperature-dependent conductivity data for ceramic samples of some of the apatite-like silicates prepared in this work. At low frequencies (10 Hz), the conductivity data are well represented by

Arrhenius-type equations. In the range 10–1000 kHz, there is a relaxation contribution, which rises rapidly with decreasing temperature.

The Arrhenius plots are essentially linear at high temperatures, 500–1000 $^\circ\text{C}$, which allows the ionic conductivity data to be fitted by Arrhenius-type equations.

Table 2. Comparison of synthesis and sintering conditions for $\text{M}_2^{\text{II}}\text{Ln}_8(\text{SiO}_4)_6\text{O}_2$ orthosilicate ceramics prepared by solid-state reactions and sol-gel processing

Process	Synthesis conditions		Sintering conditions	
	$t, ^\circ\text{C}$	τ, h	$t, ^\circ\text{C}$	τ, h
Solid-state	1400–1600	80–100	1500–1600	16
Sol-gel	1100	2	1350–1430	1

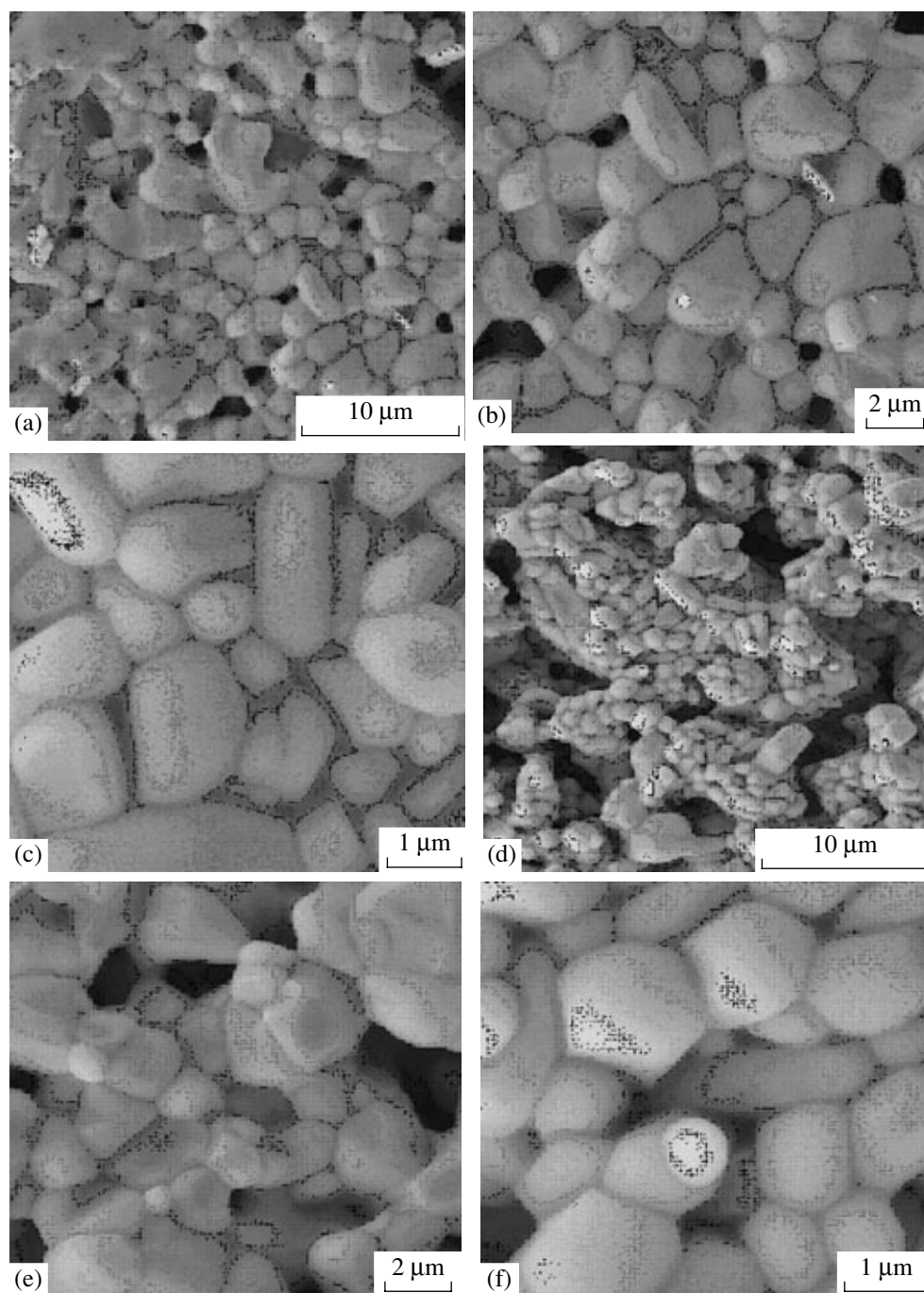


Fig. 1. Microstructures of $\text{Ca}_2\text{Nd}_8(\text{SiO}_4)_6\text{O}_2$ ceramics prepared through (a–c) sol–gel processing and (d–f) solid-state reactions.

The activation energy for ion transport through lattice sites was evaluated using the relation $\sigma T = \sigma_0 \exp(-E_a/T)$. The activation energies thus found (Table 1) are about 1 eV, in agreement with those reported by Masubuchi *et al.* [12] and Sansom *et al.* [13] for oxygen-ion transport. Characteristically, the 900°C conductivity of our ceramics is only slightly lower than that of single crystals [12].

According to their conductivity, the ceramics can be divided into four groups: $\text{Ln}_{9.33}(\text{SiO}_4)\text{O}_2$ (I), $\text{Pb}_2\text{Ln}_8(\text{SiO}_4)_6\text{O}_2$ (II), $\text{Sr}_2\text{Ln}_8(\text{SiO}_4)_6\text{O}_2$ (III), and $\text{Ca}_2\text{Ln}_8(\text{SiO}_4)_6\text{O}_2$ (IV). As seen in Fig. 3, the high-temperature conductivity exhibits Arrhenius behavior within each group. All of the lines are very close in slope, indicating that the materials differ little in activation energy (Table 1). The systematic variation in acti-

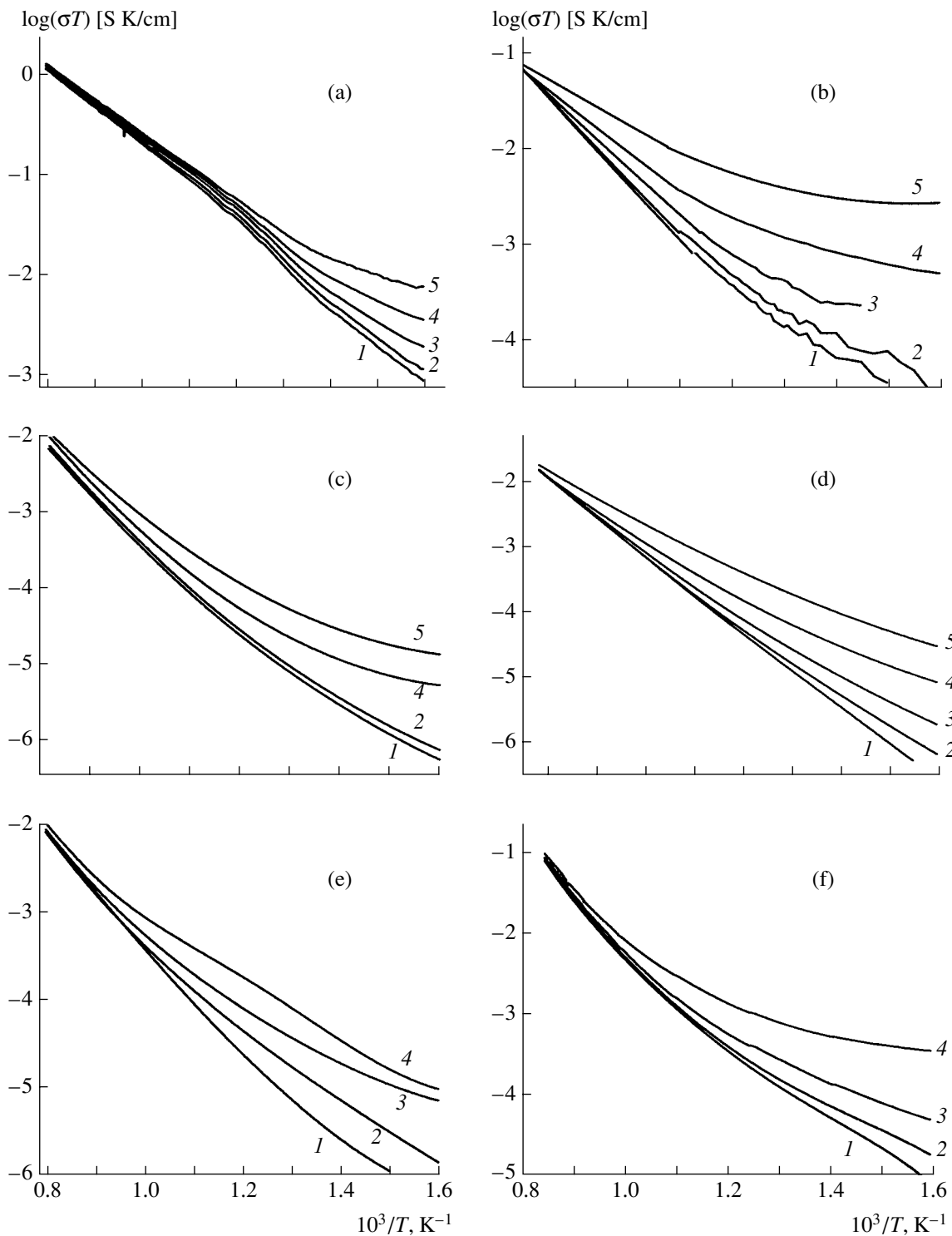


Fig. 2. Arrhenius plots of conductivity for (a) $\text{La}_{9.33}(\text{SiO}_4)_6\text{O}_2$, (b) $\text{Pb}_2\text{Er}_8(\text{SiO}_4)_6\text{O}_2$, (c) $\text{Ca}_2\text{Gd}_8(\text{SiO}_4)_6\text{O}_2$, (d) $\text{Sr}_2\text{Gd}_8(\text{SiO}_4)_6\text{O}_2$, (e) $\text{Ca}_2\text{Nd}_8(\text{SiO}_4)_6\text{O}_2$, and (f) $\text{Pb}_2\text{La}_8(\text{SiO}_4)_6\text{O}_2$ at frequencies of (1) 10, (2) 10^2 , (3) 10^3 , (4) 10^4 , and (5) 10^5 Hz.

vation energy across the $\text{M}_2^{\text{II}}\text{Ln}_8(\text{SiO}_4)_6\text{O}_2$ ($\text{Ln} = \text{La}, \text{Nd}, \text{Gd}, \text{Er}$) series indicates that, at a given M^{II} , the potential barrier to oxygen-ion transport decreases with an increase in the size of Ln cations. In addition, the

barrier height decreases in going from Ca to Sr and to Pb, i.e., with increasing cation size.

Figure 4 presents temperature-dependent conductivity data for a silicophosphate containing one PO_4 group

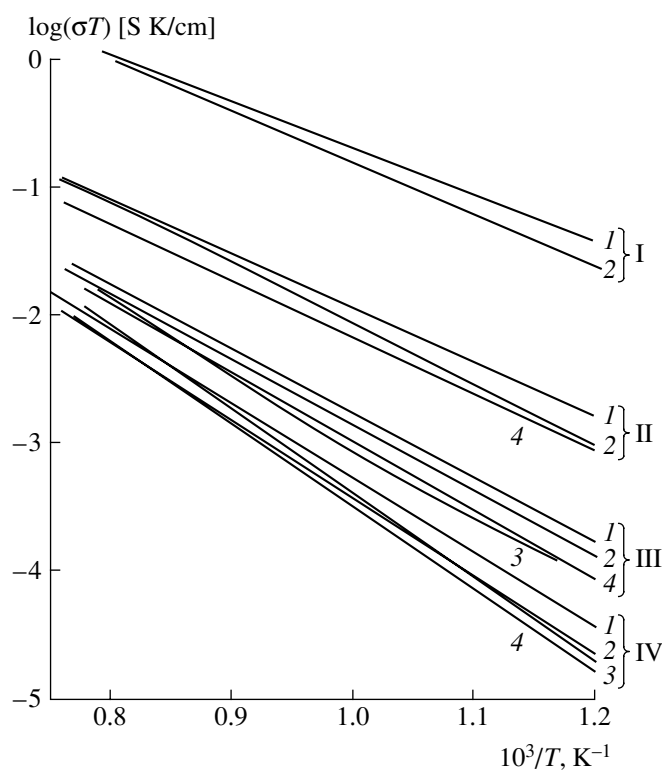


Fig. 3. Arrhenius plots of conductivity for four groups of ceramics: (I) $\text{Ln}_{9.33}(\text{SiO}_4)_6\text{O}_2$, (II) $\text{Pb}_2\text{Ln}_8(\text{SiO}_4)_6\text{O}_2$, (III) $\text{Sr}_2\text{Ln}_8(\text{SiO}_4)_6\text{O}_2$, and (IV) $\text{Ca}_2\text{Ln}_8(\text{SiO}_4)_6\text{O}_2$; Ln = (1) La, (2) Nd, (3) Gd, (4) Er.

per formula unit. It is of interest to note that the replacement of the silicon atom in an SiO_4 tetrahedron with a (smaller sized) phosphorus atom (e.g., in $\text{La}_7\text{Ca}_3(\text{SiO}_4)_5(\text{PO}_4)\text{O}_2$) has little or no effect on ionic transport, as follows from the data in Fig. 4 in comparison with the analogous data for silicates (Fig. 2). Nevertheless, such substitutions are of interest because they can be used to maintain electroneutrality between the anion and cation sublattices while reducing the content of large-sized cations. This may lead to an increase in oxygen ionic conductivity in going to more phosphorus-rich compositions, e.g., $\text{La}_{9.33}(\text{SiO}_4)_4(\text{PO}_4)_2\text{O}_3$ and $\text{La}_6(\text{SiO}_4)_5(\text{PO}_4)\text{O}_2$. In this study, attempts to synthesize such compounds in single-phase form were unsuccessful, but it makes sense to continue efforts along these lines since the cation-deficient materials $\text{Ln}_{9.33}(\text{SiO}_4)_6\text{O}_2$ (Ln = La, Nd) offer the highest 900°C oxygen ionic conductivity among the materials studied here, $\sim 10^{-3}$ S/cm (Fig. 3), in agreement with earlier findings [12, 13].

In addition, we measured the temperature-dependent dielectric permittivity of the synthesized orthosilicates and silicophosphates (Fig. 5). The results demonstrate that ϵ is a monotonic function of temperature. The relatively low values of ϵ and the absence of anomalies in both the heating and cooling curves for all of the compounds studied suggests that they undergo no

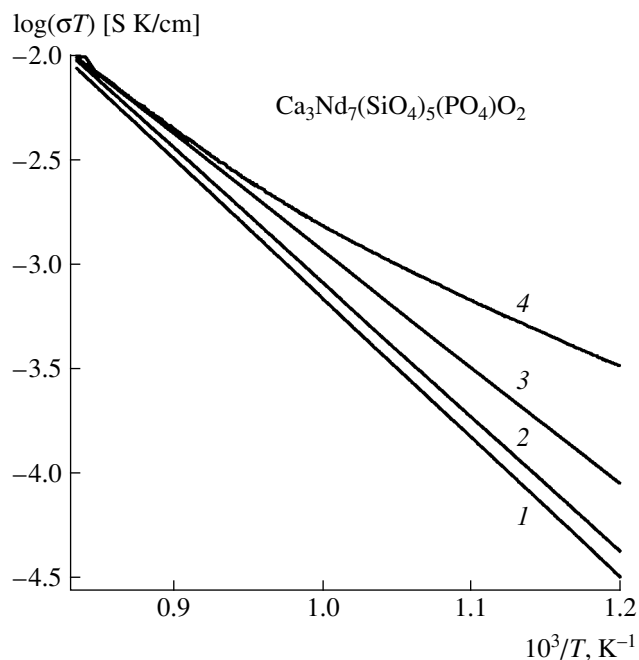


Fig. 4. Arrhenius plots of low-frequency conductivity for apatite-structure calcium neodymium silicophosphate: $f =$ (1) 10, (2) 100, (3) 500, (4) 1000 Hz.

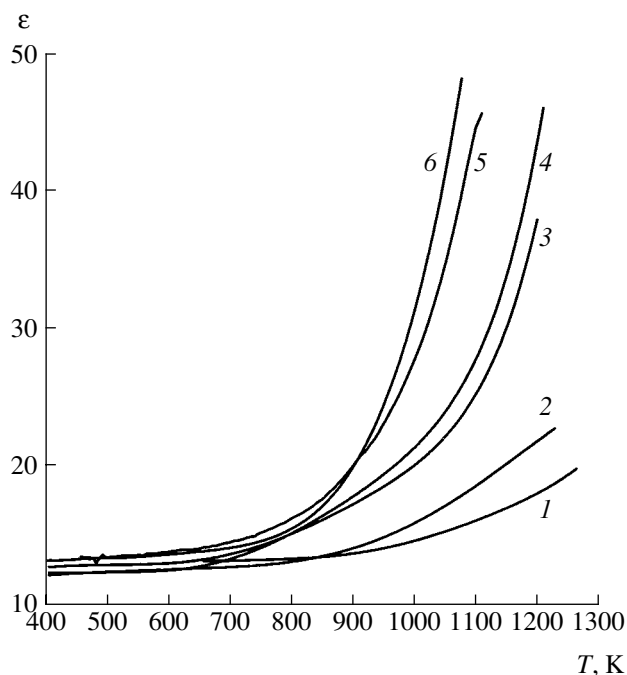


Fig. 5. Temperature dependences of 100-kHz permittivity for (1) $\text{La}_{9.33}(\text{SiO}_4)_6\text{O}_2$, (2) $\text{Nd}_{9.33}(\text{SiO}_4)_6\text{O}_2$, (3) $\text{Pb}_2\text{La}_8(\text{SiO}_4)_6\text{O}_2$, (4) $\text{Pb}_2\text{Er}_8(\text{SiO}_4)_6\text{O}_2$, (5) $\text{Sr}_2\text{La}_8(\text{SiO}_4)_6\text{O}_2$, and (6) $\text{Sr}_2\text{Gd}_8(\text{SiO}_4)_6\text{O}_2$.

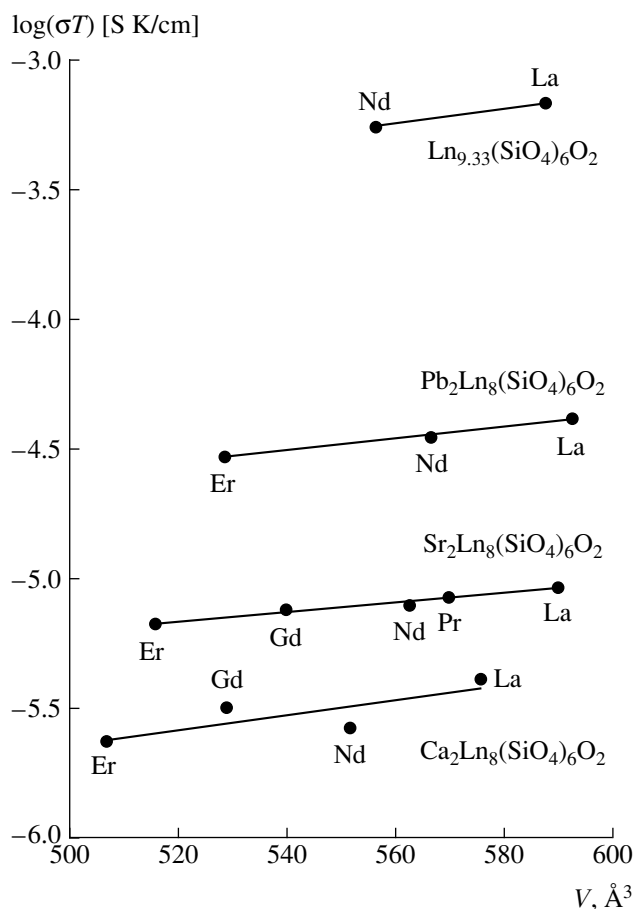


Fig. 6. 900°C oxygen ionic conductivity as a function of unit-cell volume for apatite-structure silicates.

phase transitions, which is attractive for practical application of these materials.

One feature of crystal-chemical interest is that the conductivity of the oxosilicates $\text{Ca}_2\text{La}_8(\text{SiO}_4)_6\text{O}_2$, $\text{Sr}_2\text{La}_8(\text{SiO}_4)_6\text{O}_2$, and $\text{Pb}_2\text{La}_8(\text{SiO}_4)_6\text{O}_2$ is one to two orders of magnitude lower than that of the cation-deficient silicates $\text{Ln}_{0.33}(\text{SiO}_4)_6\text{O}_2$. Cation deficiency seems to be essential for the transport of oxygens that are not incorporated into SiO_4 groups along the channels between the large-sized, alkaline-earth and rare-earth cations. On the other hand, as seen in Fig. 6, the conductivity of the compounds under consideration increases with the average size of these cations. This is attributable to the increase in unit-cell dimensions and, hence, in free volume, which, as a rule, leads to a rise in ionic conductivity.

The fact that our ceramics are close in conductivity to single-crystal analogs attests to high structural perfection of the ceramics and indicates that sol-gel processing has great potential for the synthesis of oxygen-ion conducting orthosilicate-based solid electrolytes. Comparison of the synthesis and sintering conditions in solid-state and sol-gel processes (Table 2) highlights

the important advantages of the latter: a manifold reduction in process duration and a reduction in sintering temperature by 200–300°C.

CONCLUSIONS

We prepared apatite-structure solid solutions and measured their electrical conductivity. The conductivity of the $\text{M}_2\text{Ln}_8(\text{SiO}_4)_6\text{O}_2$ ceramics was found to be close to that reported earlier for oxygen-ion-conducting single crystals, which attests to high structural perfection of the ceramics and indicates that sol-gel processing has great potential for the synthesis of orthosilicate-based materials for ionic-membrane applications.

ACKNOWLEDGMENTS

We are grateful to V.I. Putlyaev for the electron-microscopic examination of the surface of the ceramic samples.

This work was supported by the Russian Foundation for Basic Research, project no. 04-03-33091.

REFERENCES

1. Brian, C.H. and Heinzl, A., Materials for Fuel-Cell Technologies, *Nature*, 2001, vol. 414, no. 2, pp. 345–352.
2. Steele, B.C.H., Oxygen Ion Conductors, *High Conductivity Solid Ionic Conductors, Recent Trends and Applications*, Takahashi, T.T., Ed., Singapore: World Scientific, 1989, pp. 402–446.
3. Stoukides, M., Applications of Solid Electrolytes in Heterogeneous Catalysis, *Ind. Eng. Chem. Res.*, 1988, vol. 27, no. 10, pp. 1745–1750.
4. Steele, B.C.H., Material Science and Engineering: The Enabling Technology for the Commercialization of Fuel Cell Systems, *J. Mater. Sci.*, 2001, vol. 36, no. 4, pp. 1053–1068.
5. Boivin, J.C. and Mairesse, G., Recent Material Developments in Fast Oxide Ion Conductors, *Chem. Mater.*, 1998, vol. 10, pp. 2870–2888.
6. Turova, N.Ya., Turevskaya, E.P., Kessler, V.G., and Yanovskaya, M.I., *The Chemistry of Metal Alkoxides*, Dordrecht: Kluwer, 2002.
7. Michael, D., Prez, M., Jorba, Y., and Collongues, R., Etude de la transformation ordre-désordre de la structure fluorite à la structure pyrochlore pour des phases $(1-x)\text{ZrO}_2\text{Ln}_2\text{O}_3$, *Mater. Res. Bull.*, 1974, vol. 9, pp. 1457–1468.
8. Feng, M. and Goodenough, J.B., A Superior Oxide-Ion Electrolyte, *Solid State Inorg. Chem.*, 1994, vol. 31, pp. 663–672.
9. Huang, P. and Petric, A., Superior Oxygen Ion Conductivity of Lanthanum Gallate Doped with Strontium and Magnesium, *J. Electrochem. Soc.*, 1996, vol. 143, pp. 1644–1648.

10. Huang, K., Tichy, R.S., and Goodenough, J.B., Superior Perovskite Oxide-Ion Conductor; Strontium- and Magnesium-Doped LaGaO₃: I. Phase Relationships and Electrical Properties, *J. Am. Ceram. Soc.*, 1998, vol. 81, pp. 2565–2575.
11. Thomas, I.M., *Sol–Gel Technology for Thin Films, Fibers, Preforms, Electronics, and Specialty Shapes*, Klein, L.C., Ed., Noyes Park Ridge, 1988, p. 2.
12. Masubuchi, Y., Higuchi, M., Katase, H., *et al.*, Oxide Ion Conduction in Nd_{9.33}(SiO₄)₆O₂ and Sr₂Nd₈(SiO₄)₆O₂ Single Crystals Grown by Floating Zone Method, *Solid State Ionics*, 2004, vol. 166, pp. 213–217.
13. Sansom, J.E.H., Richings, D., and Slater, P.R., A Powder Neutron Diffraction Study of the Oxide-Ion-Conducting Apatite-Type Phases, La_{9.33}Si₆O₂₆ and La₈Sr₂Si₆O₂₆, *Solid State Ionics*, 2001, vol. 139, pp. 205–210.
14. Turova, N.Ya. and Novoselova, A.V., Solubility of Magnesium Alkoxides and Alkaline-Earth Metals in Alcohols, *Izv. Akad. Nauk SSSR, Neorg. Mater.*, 1967, vol. 3, no. 2, pp. 351–360.
15. Rakhomovsky, Ya.A., Menshikov, Yu.R., Yakovenshuk, V.N., *et al.*, Cerite-(Ia), (La,Ce,Ca)₉(Fe,Ca,Mg)(SiO₄)₃(SiO₃(OH))₄(OH)₃, a New Mineral from the Khibiny Alkaline Massif: Occurrence and Crystal Structure, *Materialy 4-go mezhdunarodnogo simpoziuma mineralogicheskikh muzeev* (Proc. 4th Int. Symp. of Mineralogical Museums), St. Petersburg, 2002, p. 271.